

# Kinetics and Mechanism of the Nucleophilic Substitution Reaction of Imidazole with Bis(2,4,6-trichlorophenyl) Oxalate and Bis(2,4-dinitrophenyl) Oxalate

Andrew G. Hadd and John W. Birks\*

Department of Chemistry and Biochemistry and Cooperative Institute for Research in Environmental Science (CIRES), University of Colorado, Boulder, Colorado 80309-0216

Received September 6, 1995<sup>®</sup>

The kinetics of the imidazole-catalyzed decomposition of bis(2,4,6-trichlorophenyl) oxalate (TCPO) and bis(2,4-dinitrophenyl) oxalate (DNPO) was investigated by the stopped-flow technique. Pseudo-first-order rate constants were determined as a function of imidazole concentration in the temperature range 6–45 °C by fitting the temporal changes in absorbance throughout the 245 to 345 nm wavelength range for TCPO and at 420 nm for DNPO. The reaction proceeds by release of two molecules of substituted phenol and formation of 1,1'-oxalyldiimidazole (ODI) for both esters. The identity of ODI was confirmed in the reaction of imidazole with TCPO by its UV absorbance spectrum and <sup>13</sup>C-NMR spectrum. The reaction of imidazole with TCPO has a second-order dependence on imidazole concentration and an observed negative activation energy of  $-6.2 \pm 0.3$  kJ/mol, whereas the DNPO reaction has a first-order dependence on imidazole concentration and an observed positive activation energy of  $12.0 \pm 0.6$  kJ/mol. The differences in the temperature dependence and order of the reaction with respect to imidazole for the two oxalate esters are explained by a shift in the rate-determining step from addition to the acyl group for DNPO to imidazole-catalyzed release of the phenol leaving group for TCPO. These kinetics results are useful in interpreting the initial reaction steps in peroxyoxalate chemiluminescence.

## Introduction

In peroxyoxalate chemiluminescence (PO-CL), an aryl oxalate ester reacts with hydrogen peroxide in the presence of a fluorophore to generate light. The PO-CL reaction has become a widely used analytical tool for trace analysis,<sup>1,2</sup> and in a number of cases a 10- to 100-fold increase in sensitivity over conventional fluorescence detection has been demonstrated.<sup>3–5</sup> Several authors have investigated the kinetics and mechanism of the PO-CL reaction.<sup>6–11</sup> Although several features of the mechanism have been explored, the key pathway(s) and nature of the reactive intermediate(s) remain highly uncertain. We are exploring the reaction kinetics and mechanism of peroxyoxalate chemiluminescence in order to evaluate the possibility of detecting single molecules. This paper explores the use of the common PO-CL catalyst, imidazole, and its effect on the rate-determining steps of the light-generating reaction.

The peroxyoxalate chemiluminescence reaction is accelerated by the presence of a weak base, with imidazole (ImH) having the greatest effect on the chemiluminescence yield and kinetics.<sup>10</sup> The PO-CL reaction has been

shown to have a first- and second-order dependence on the imidazole concentration, and this effect has been attributed to concurrent "nucleophilic" and "general-base" catalysis by imidazole.<sup>11</sup> Additionally, Alvarez *et al.* have suggested that the nature and concentration of the catalyst affects the formation of different intermediates in the PO-CL reaction.<sup>8</sup> However, the catalytic role of imidazole and its effect on the formation of intermediates in the PO-CL reaction has not been well characterized.

The imidazole-catalyzed hydrolysis of esters bearing good leaving groups is known to proceed by a nucleophilic-catalysis pathway.<sup>12–14</sup> For example, the intermediate formation of *N*-acetylimidazole has been observed for the imidazole-catalyzed hydrolysis of *p*-nitrophenyl acetate.<sup>15</sup> Recently, Neuvonen has examined the neutral and imidazole-catalyzed hydrolysis of bis(4-nitrophenyl) oxalate (4-NPO).<sup>16</sup> The imidazole-catalyzed degradation of 4-NPO was found to proceed by the successive release of two 4-nitrophenyl groups with rapid formation of 1,1'-oxalyldiimidazole (ODI). Neuvonen suggested that ODI is the dominant intermediate in the PO-CL reaction.

ODI itself has been used for the chemiluminescence detection of hydrogen peroxide in the presence of a fluorophore.<sup>17</sup> The uncatalyzed reaction of ODI with hydrogen peroxide was found to have faster kinetics but similar quantum yields when compared to the imidazole-catalyzed reaction of bis(2,4,6-trichlorophenyl) oxalate (TCPO) with hydrogen peroxide. In spite of these studies, the intermediacy of ODI in peroxyoxalate chemilumines-

<sup>®</sup> Abstract published in *Advance ACS Abstracts*, April 1, 1996.

(1) Hadd, A. G.; Birks, J. W. in *Peroxyoxalate Chemiluminescence: Mechanism and Analytical Detection*; Sievers, R. E., Ed.; John Wiley and Sons: New York, 1995; pp 209–239.

(2) Robards, K.; Worsfold, P. J. *Anal. Chim. Acta* **1992**, *266*, 147–173.

(3) Kobayashi, S.; Imai, K. *Anal. Chem.* **1980**, *52*, 424.

(4) Sigvardson, K. W.; Birks, J. W. *Anal. Chem.* **1983**, *55*, 432–435.

(5) Mellbin, G.; Smith, B. E. F. *J. Chromatogr.* **1984**, *312*, 203.

(6) Rauhut, M. M. *Acc. Chem. Res.* **1969**, *2*, 80–87.

(7) Catherall, C. L.; Palmer, T. F.; Cundall, R. B. *J. Chem. Soc., Faraday Trans. 2* **1984**, *80*, 837–849.

(8) Alvarez, F. J.; Parekh, N. J.; Matuszewski, B.; Givens, R. S.; Higuchi, T.; Schowen, R. L. *J. Am. Chem. Soc.* **1986**, *108*, 6435–6437.

(9) Milofsky, R. E.; Birks, J. W. *J. Am. Chem. Soc.* **1991**, *113*, 9715–9723.

(10) Hanaoka, N.; Givens, R. S.; Schowen, R. L.; Kuwana, T. *Anal. Chem.* **1988**, *60*, 2193–2197.

(11) Orlovic, M.; Schowen, R. L.; Givens, R. S.; Alvarez, F.; Matuszewski, B.; Parekh, N. *J. Org. Chem.* **1989**, *54*, 3605.

(12) Bruce, T. C.; Schmir, G. L. *J. Am. Chem. Soc.* **1956**, *76*, 1663–1667.

(13) Kirsch, J. F.; Jencks, W. P. *J. Am. Chem. Soc.* **1984**, *86*, 833–837.

(14) Neuvonen, H. *J. Chem. Soc., Perkin Trans 2* **1995**, 951.

(15) Bender, M. L.; Turnquest, B. W. *J. Am. Chem. Soc.* **1957**, *79*, 1652–1655.

(16) Neuvonen, H. *J. Chem. Soc. Perkin Trans. 2* **1995**, 945.

(17) Stigbrand, M.; Ponten, E.; Irgum, K. *Anal. Chem.* **1994**, *66*, 1766.

cence has not been fully established. Since single molecule detection would require the production of high concentrations of the reactive intermediate(s) responsible for the energy transfer to the analyte molecule, clarifying the identity and relative contributions of different intermediates is important.

In addition to the formation of ODI as a possible intermediate in the PO-CL reaction, the two oxalate esters TCPO and DNPO undergo very different hydrolysis reactions. The hydrolysis of DNPO results in the rapid decarbonylation and decarboxylation of the aryl hydrogen oxalate without formation of oxalic acid.<sup>18–20</sup> Although the much faster kinetics of DNPO and different hydrolysis mechanism has been explored, further work comparing common oxalate esters could provide additional insight necessary for developing a general peroxyoxalate chemiluminescence mechanism.

We investigated the isolated reactions of TCPO and DNPO with imidazole in order to better understand the first of several key steps leading to chemiluminescence. The kinetics of the reaction was studied using the stopped-flow technique to monitor temporal changes in the ultraviolet (UV) absorption spectrum. Reaction conditions were chosen with imidazole in large excess over each ester, and pseudo-first-order rate constants were obtained as a function of imidazole concentration and temperature. <sup>13</sup>C-NMR was used to aid in identifying the intermediate formed in the reaction of TCPO.

### Experimental Section

**Chemicals.** Bis(2,4,6-trichlorophenyl) oxalate, imidazole, triethylamine, 2,4,6-trichlorophenol (TCP), bis(2,4-dinitrophenyl) oxalate, 2,4-dinitrophenol (DNP), and 1,1'-oxalyldiimidazole (technical grade, ≥90% with principal impurity being imidazole) were purchased from Aldrich. Burdick and Jackson HPLC-grade acetonitrile was used for all dilutions and experiments. Chemicals and solvents were used without further purification. Stock solutions of 0.10 M imidazole, 2.0 mM TCPO, and 2.0 mM DNPO were prepared and stored in the dark prior to dilution and analysis. Fresh DNPO solutions were prepared every 6 h.

**Kinetics Measurements.** A Hewlett-Packard 8452 diode array spectrometer was used to determine the UV absorption spectra of each of the reagents and possible products. Stopped-flow measurements were made using an Applied Photophysics DX-17MV stopped-flow spectrophotometer (Applied Photophysics, Leatherhead, UK) thermostated by a circulating water bath. In a typical experiment, one syringe of the stopped-flow instrument was filled with 0.20 mM TCPO in acetonitrile and the other syringe filled with 5.0, 10.0, 15.0, or 20.0 mM imidazole, also in acetonitrile. After 1:1 mixing of the reagents, absorbance versus time data were collected in the range of 245 to 345 nm in 5-nm intervals over 1000 s. Three-dimensional plots of absorbance, wavelength, and time were analyzed using a global nonlinear regression fitting program, GLINT, available from Applied Photophysics. Each data fit utilized a minimum of 1000 data points at each wavelength. The kinetics of the reaction of DNPO (0.020 mM, final concentration) with imidazole (0.5 to 2.0 mM, final concentration) was determined by following the dinitrophenol absorbance at 420 nm for 0.5 s. All reported rate constants are tabulated using postmixing reagent concentrations.

**<sup>13</sup>C-Nuclear Magnetic Resonance Measurements (<sup>13</sup>C-NMR).** A Varian VXR-300S nuclear magnetic resonance spectrometer was used to obtain <sup>13</sup>C-NMR spectra. Imidazole, 0.10 g, was added to 0.05 g of TCPO dissolved in 15 mL of

CDCl<sub>3</sub>. After 5 min, the solvent was partially evaporated under vacuum. NMR spectra were recorded over a 2-h period.

### Results

**Effect of Imidazole Concentration on the Spectra of 2,4,6-Trichlorophenol and 2,4-Dinitrophenol.** Deprotonation of phenols results in a characteristic shift in the absorbance spectrum to longer wavelengths. In order to investigate the ability of imidazole to deprotonate each phenol, absorbance spectra were determined in acetonitrile as a function of added imidazole, as shown in Figure 1. The spectra show only a small increase in phenolate absorbance at 320 nm upon addition of imidazole to TCP (Figure 1a). By comparison, in a 50/50 by volume mixture of water and MeCN, there is a very large increase in trichlorophenolate absorbance at 320 nm with increasing imidazole concentration. In the case of DNP, intense absorption bands grow in at 380 and 425 nm upon addition of imidazole in neat MeCN (Figure 1b), indicating a large degree of ionization. From these results it is concluded that in acetonitrile the relative p*K*<sub>a</sub>'s are DNP < ImH<sub>2</sub><sup>+</sup> < TCP.

**TCPO Reaction Kinetics and Spectra of Reaction Products and Intermediates.** The reaction of TCPO with an excess of imidazole was monitored in the 245 to 345 nm wavelength range as a function of imidazole concentration and temperature. An example of a three-dimensional time, wavelength, and absorbance plot is shown in Figure 2. Pseudo-first-order rate constants were determined using the simplified reaction model



The experimental data fit this model well and were used to calculate the spectra of the intermediate B and phenol product P. The rate constants were derived by monitoring the array of molar absorptivity changes of the calculated spectra over time. The rate constant *k*<sub>a</sub> follows essentially the increase in the phenol absorbance, and *k*<sub>b</sub> the decrease in the absorbance of intermediate B. The calculated spectrum of P matched a standard spectrum of 2,4,6-trichlorophenol well within experimental error at each temperature and imidazole concentration. Attempts to model the reaction and follow the kinetics using the stepwise addition of imidazole were unsuccessful. Apparently, the second imidazole substitution is very fast in comparison to the first substitution.

The derived first-order rate constants as a function of imidazole concentration and temperature are given in Table 1 for *k*<sub>a</sub> and Table II for *k*<sub>b</sub>. The rate constant *k*<sub>a</sub> is strongly affected by the imidazole concentration. A plot of the pseudo-first-order rate constant versus imidazole concentration for a temperature of 24.7 °C is provided in Figure 3. The rate constants were fit to a second-order polynomial, resolving the pseudo-first-order rate constant into zero-, first-, and second-order contributions according to the equation:

$$k_a = a + b[\text{ImH}] + c[\text{ImH}]^2 \quad (2)$$

The second-order term dominates the reaction kinetics, and the reaction approximately follows the rate equation:

$$k_a = c[\text{ImH}]^2 \quad (3)$$

An Arrhenius plot of the third-order (first order in TCPO, second order in ImH) rate coefficient, *c* (eq. 2), is

(18) Jennings, R. N.; Capomacchia, A. C. *Anal. Chim. Acta* **1988**, *205*, 207.

(19) Orosz, G.; Dudar, E. *Anal. Chim. Acta* **1991**, *247*, 141–147.

(20) Neuvonen, H. *J. Chem. Soc., Perkin Trans. 2* **1994**, 89.

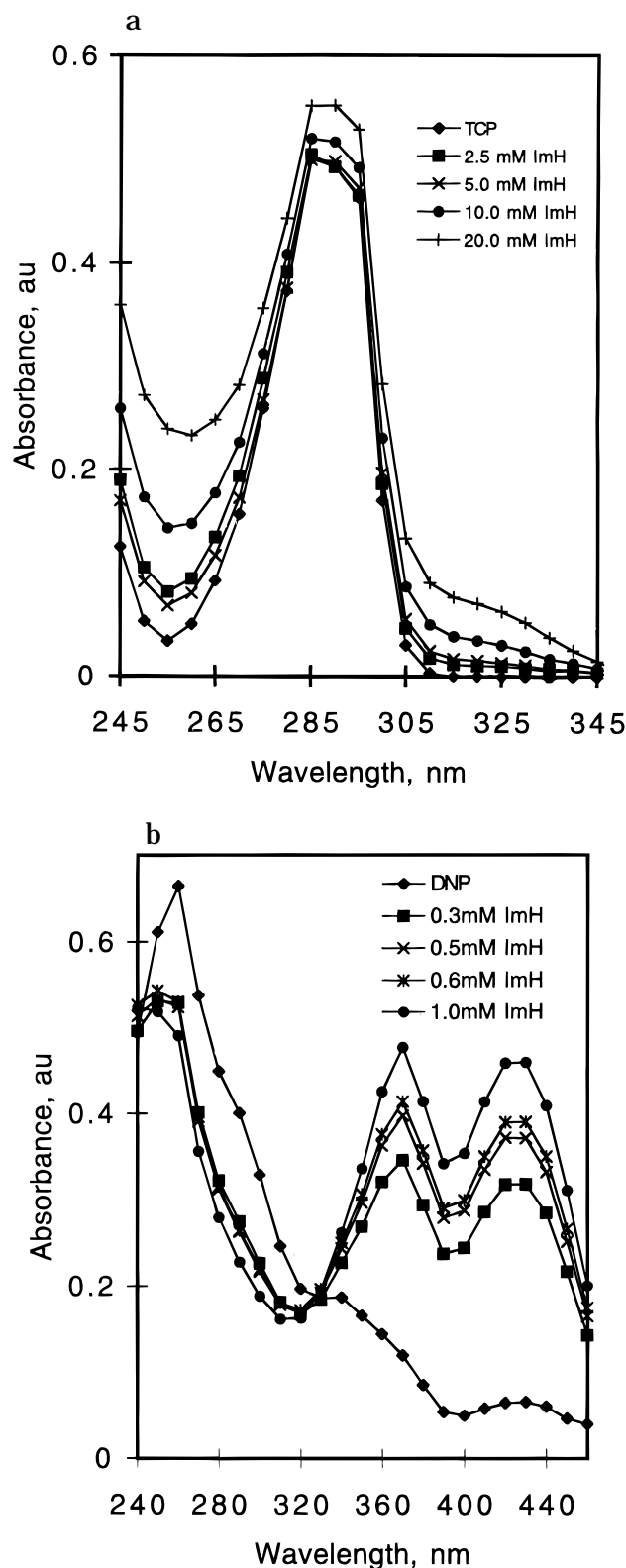


**Figure 1.** Effect of imidazole concentration on the absorption spectra of 2,4,6-trichlorophenol (a) and 2,4-dinitrophenol (b) in acetonitrile.

given in Figure 4 and displays an observed negative activation energy of  $-6.2 \pm 0.3$  kJ/mol.

The absorption spectrum of intermediate B (eq 1) was calculated from temporal changes in the molar absorptivities over the wavelength range 245 to 345 nm using the GLINT program. This spectrum is compared with a standard spectrum of 1,1'-oxalyldiimidazole in Figure 5. The spectra agree extremely well in shape, and differ-

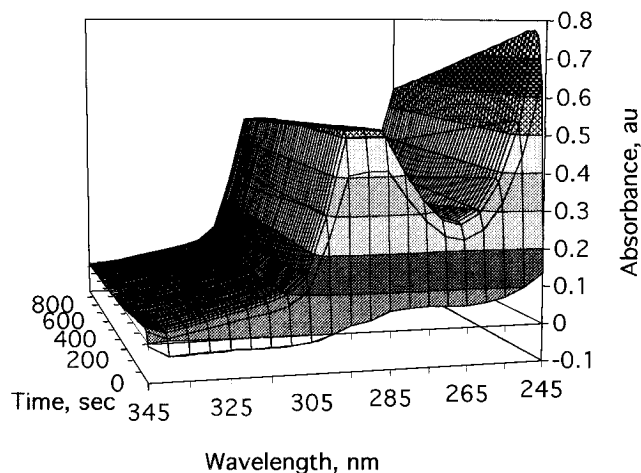


**Figure 2.** Example of an absorbance and wavelength versus time plot obtained from monitoring the reaction of imidazole with TCPO. Conditions: 5.0 mM ImH and 0.10 mM TCPO at 25 °C.

ences in absolute values between the intermediate and ODI can be attributed to calculational errors and impurities in the ODI standard of up to 10% at each wavelength. A  $^{13}\text{C}$ -NMR spectrum of the reaction mixture of TCPO with an excess of imidazole resulted in the following resonances that differed from 2,4,6-trichlorophenol and imidazole: 117.6, 130.3, 139.4, 154.7, 163.3, 163.7 ppm. The first four signals correspond to the  $^{13}\text{C}$ -NMR spectrum of an authentic sample of ODI. The remaining two signals are probably due to subsequent decomposition products formed in the slow second step of reaction 1 ( $\text{B} \rightarrow \text{C}$ ).

The effect of temperature and imidazole concentration on the decomposition rate of a commercial sample of ODI are summarized in Table 3. ODI is known to decompose into imidazole and carbon monoxide,<sup>17</sup> but product identification was not performed in this study. Qualitatively, the trend of increasing reaction rate with increasing temperature and imidazole concentration for the rate constants given in Tables 2 ( $k_b$  for the reaction of TCPO with ImH) and 3 agree. However, the rate constants in Table 2 are generally twice as fast as for a commercial sample of ODI. The two reaction systems differ in that TCP is generated in the reaction of TCPO with ImH but is not present in the ODI sample.

**DNPO Reaction Kinetics.** Table 4 contains the pseudo-first-order rate constants determined from the appearance of 2,4-dinitrophenol at 420 nm for the reaction of DNPO with imidazole. Rate constants recorded in the table were determined using a fit to a single exponential rise. The pseudo-first-order rate constants increase linearly with increasing imidazole concentration at each temperature, as seen in Figure 6. The slopes of the pseudo-first-order rate constants as a function of imidazole concentration were calculated using a linear least-squares fit. The slope corresponds to the second-order (first order in DNPO, first order in ImH) rate constant, and an Arrhenius plot for the reaction is provided as Figure 7. A positive activation energy for the reaction of DNPO with imidazole of  $12.0 \pm 0.6$  kJ/mol is obtained.

At 0.5 and 1.0 mM imidazole concentration, an improvement to the residuals was achieved using a biexponential fit to the rise, which resolves the stepwise release of both 2,4-dinitrophenolate ions. However, the

**Table 1. Pseudo-First Order Rate Constant,  $k_a$ , as a Function of Imidazole Concentration and Temperature for TCPO.<sup>a</sup> TCPO Final Concentration of 0.10 mM**

temp (°C)	[ImH], mM			
	2.5	5.0	7.5	10.0
5.8	$4.19 \pm 0.05 \times 10^{-2}$	$0.191 \pm 0.003$	$0.463 \pm 0.003$	$0.909 \pm 0.006$
15.1	$6.19 \pm 0.02 \times 10^{-2}$	$0.241 \pm 0.001$	$0.511 \pm 0.002$	$0.928 \pm 0.001$
24.7 <sup>b</sup>	$6.22 \pm 0.01 \times 10^{-2}$	$0.201 \pm 0.001$	$0.480 \pm 0.003$	$0.893 \pm 0.002$
35.1	$6.07 \pm 0.04 \times 10^{-2}$	$0.195 \pm 0.002$	$0.455 \pm 0.002$	$0.788 \pm 0.006$
44.7	$5.42 \pm 0.01 \times 10^{-2}$	$0.172 \pm 0.001$	$0.373 \pm 0.004$	$0.725 \pm 0.003$

<sup>a</sup> Rate constants in units of  $s^{-1}$ . <sup>b</sup> Additional rate constants shown in Figure 1: 3.5 mM ImH,  $0.100 s^{-1}$ , and 20.0 mM ImH,  $3.58 s^{-1}$ , at 24.7 °C.

**Table 2. Pseudo-First-Order Rate Constant,  $k_b$ , as a Function of Imidazole Concentration and Temperature for TCPO.<sup>a</sup> TCPO Final Concentration of 0.10 mM**

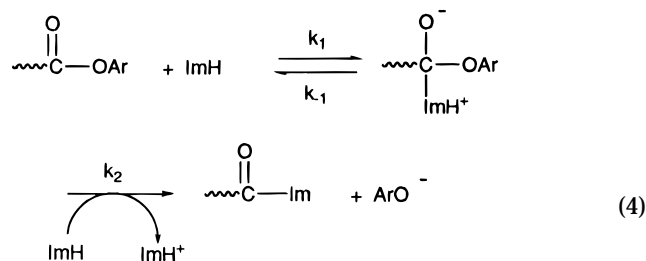
temp (°C)	[ImH], mM			
	2.5	5.0	7.5	10.0
5.8	$0.60 \pm 0.01$	$0.81 \pm 0.05$	$0.96 \pm 0.05$	$0.91 \pm 0.03$
15.1	$0.52 \pm 0.01$	$0.913 \pm 0.001$	$1.18 \pm 0.01$	$1.29 \pm 0.01$
24.7	$0.62 \pm 0.01$	$0.782 \pm 0.001$	$1.44 \pm 0.03$	$1.50 \pm 0.05$
35.1	$0.78 \pm 0.03$	$1.17 \pm 0.01$	$1.29 \pm 0.01$	$1.67 \pm 0.01$
44.7	$1.40 \pm 0.01$	$1.60 \pm 0.01$	$3.00 \pm 0.004$	$3.20 \pm 0.003$

<sup>a</sup> Rate constants in units of  $10^{-3} s^{-1}$ .

two-exponential contribution could not be resolved for trends within the entire imidazole concentration and temperature range explored. The data presented in Table 4 are thus an approximation of the kinetics of the slowest step, i.e., the release of the second phenol.

### Discussion

A general mechanism for the nucleophilic reaction of imidazole with an oxalate ester is shown below, with the understanding that the same details of the first phenol substitution also apply to the second substitution.



The mechanism begins with a pre-equilibrium step in which ImH adds to one of the carbonyls to form a zwitterionic, tetrahedral intermediate. In aprotic solvents the expulsion of the neutral amine is favored over expulsion of the negative phenoxide ion, making the reverse of the addition reaction highly favored in the absence of a base catalyst. A second imidazole molecule may act as a general-base catalyst by accepting a proton from the acylimidazolium ion and causing the release of the phenoxide ion. Applying the steady-state approximation to the tetrahedral intermediate, the derived rate law is given by

$$\text{rate} = k_1 k_2 [\text{Ox-OAr}] [\text{ImH}]^2 / (k_{-1} + k_2 [\text{ImH}]) \quad (5)$$

Depending on the values of the rate constants  $k_{-1}$  and  $k_2$ , the reaction will be either first- or second-order in imidazole concentration. For  $k_{-1} \ll k_2 [\text{ImH}]$  (i.e., rate-limiting step is addition of ImH to the carbonyl), the reaction is first-order in ImH, and for  $k_{-1} \gg k_2 [\text{ImH}]$  (i.e., a pre-equilibrium with the rate-limiting step being imi-

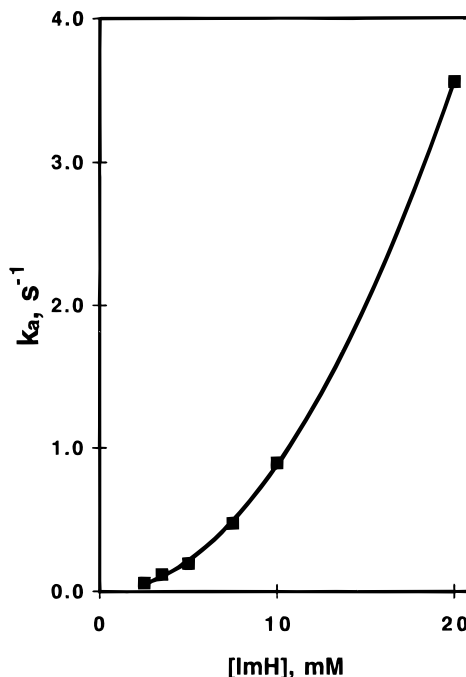


**Figure 3.** Effect of imidazole concentration on the pseudo-first-order rate constant ( $k_a$ ) for the reaction of TCPO with imidazole. Conditions: Final concentrations of 0.10-mM TCPO and 2.5 to 20.0 mM imidazole at 25 °C.

dazole-catalyzed decomposition of the tetrahedral intermediate), the reaction is second-order in ImH:

$$\text{rate} = k_1 [\text{Ox-OAr}] [\text{ImH}] \quad k_{-1} \ll k_2 [\text{ImH}] \quad (6)$$

$$\text{rate} = k_2 K_1 [\text{Ox-OAr}] [\text{ImH}]^2 \quad k_2 [\text{ImH}] \gg k_{-1} \quad (7)$$

where Ox-OAr is the oxalate ester and  $K_1 = k_1/k_{-1}$ .

The substituents and relative  $pK_a$ 's of the leaving groups will affect the relative rates of the three reaction steps, as quantified by  $k_1$ ,  $k_{-1}$ , and  $k_2$ . An electron-withdrawing substituent in the leaving group shifts the equilibrium ( $k_1/k_{-1}$ ) of reaction 4 to the right by promoting addition of the amine,<sup>21</sup> the inductive effect of DNP being greater than that of TCP. The rate of decomposition of the tetrahedral intermediate depends on the  $pK_a$  of the leaving group. DNP is much more acidic than TCP in water ( $pK_a$ 's of 4.08 and 7.42),<sup>22,23</sup> dimethyl furan ( $pK_a$ 's of 6.4 and 12.4),<sup>24</sup> dimethyl sulfoxide ( $pK_a$ 's of 5.1 and 10.2),<sup>24</sup> and propylene carbonate ( $pK_a$ 's of 14.9 and 18.0).<sup>24</sup> The imidazolium ion,  $\text{ImH}_2^+$ , has  $pK_a$ 's intermediate

(21) Menger, F. M.; Smith, J. H. *J. Am. Chem. Soc.* **1972**, *94*, 3824.

(22) *Lange's Handbook of Chemistry*, 14th ed.; Dean, J. A., Ed., McGraw-Hill: New York, 1992.

(23) *Dictionary of Organic Compounds*, 5th ed.; Buckingham, J., Ed., Chapman and Hall: New York, 1982; Vol. 5.

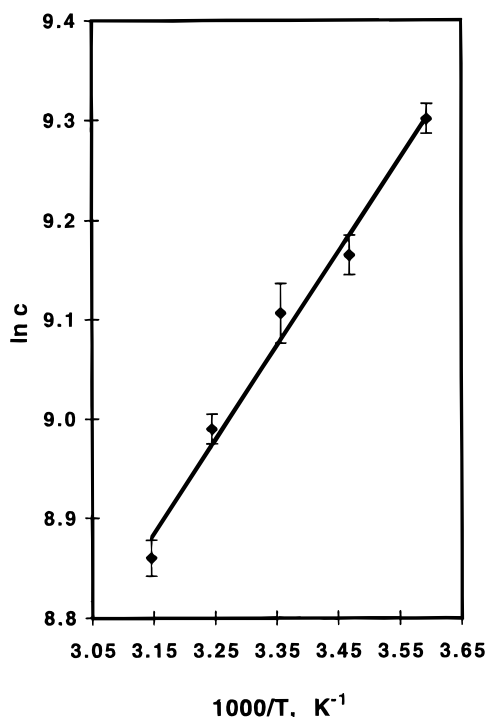


**Figure 4.** Arrhenius plot for third-order rate coefficient  $c$  (eq 2) for the reaction of ImH with TCPO.

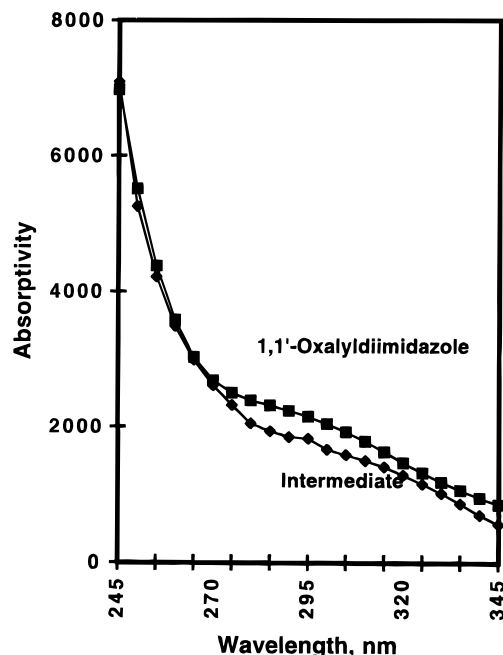


**Figure 5.** Absorption spectrum of intermediate B (eq 2) calculated by the kinetics fitting program GLINT compared with a standard spectrum of 1,1'-oxalyldiimidazole.

between those of DNP and TCP in water ( $pK_a$  of 7.0)<sup>22</sup> and in DMSO ( $pK_a$  of 6.3).<sup>23</sup> Our spectroscopic results place the  $pK_a$  of  $\text{ImH}_2^+$  intermediate between those of TCP and DNP; i.e., ImH can abstract a proton from DNP but not from TCP. Thus, the relative ease of expulsion of the leaving groups are 2,4-dinitrophenolate, followed by imidazole, followed by 2,4,6-trichlorophenolate.

The differences in reaction order with respect to ImH for the DNPO and TCPO reactions can be explained by

**Table 3.** Effect of Temperature and Imidazole Concentration on the Decomposition Kinetics of a Commercial Sample of ODI. Conditions: 0.10 mM ODI with 2.5 mM ImH at Each Temperature, and at 25 °C for Variation of Imidazole Concentration

temp, °C	$k_b, 10^{-3} \text{ s}^{-1}$	[ImH], mM	$k_b, 10^{-3} \text{ s}^{-1}$
6.8	$0.20 \pm 0.02$	2.5	$0.38 \pm 0.03$
15.1	$0.41 \pm 0.01$	5.0	$0.39 \pm 0.02$
25.0	$0.38 \pm 0.03$	10.0	$0.59 \pm 0.02$
34.6	$0.45 \pm 0.01$	15.0	$0.78 \pm 0.01$
44.6	$0.48 \pm 0.02$		

**Table 4.** Pseudo-First-Order Rate Constants as a Function of Temperature and Imidazole Concentration for DNPO Monitored at 420 nm.<sup>a</sup> Conditions: 0.02 mM DNPO Final Concentration

temp (°C)	[ImH], mM				
	0.05	1.00	1.25	1.50	2.00
6.7	$34.4 \pm 0.1$	$68.8 \pm 0.2$	$81.6 \pm 0.3$	$95.0 \pm 0.4$	$127 \pm 1$
15.0	$40.8 \pm 0.1$	$79.9 \pm 0.3$	$95.2 \pm 0.1$	$110 \pm 1$	$139 \pm 3$
25.1	$43.9 \pm 0.1$	$92.5 \pm 0.5$	$110 \pm 1$	$129 \pm 2$	$166 \pm 2$
35.0	$52.0 \pm 0.1$	$113 \pm 0.2$	$132 \pm 1$	$152 \pm 1$	$199 \pm 2$
44.6	$56.8 \pm 0.2$	$129 \pm 0.1$	$151 \pm 2$	$178 \pm 4$	$230 \pm 5$

<sup>a</sup> Rate constants in units of  $\text{s}^{-1}$ .

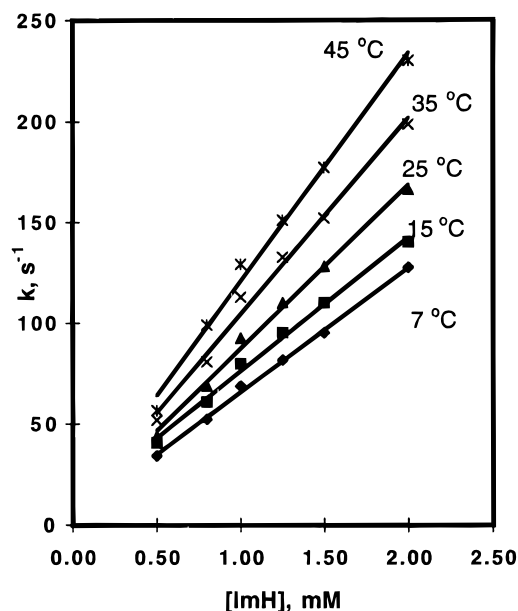


**Figure 6.** Effect of imidazole concentration on the pseudo-first-order rate constant  $k_a$  for the reaction of DNPO with ImH. Conditions: Final concentrations of 0.020 mM DNPO and 0.5 to 2.0 mM imidazole at 25 °C.

different rate-determining steps for the two reactions according to the proposed mechanism. In the case of DNPO, reaction of the tetrahedral intermediate to form products,  $k_2[\text{ImH}]$ , is fast compared to decomposition to products,  $k_{-1}$ , so that the addition reaction is the rate-limiting step and the net reaction is first-order in ImH (eq 6). For TCPO, the elimination reaction is slow compared to decomposition of the tetrahedral intermediate, with the result that the reaction is second order in ImH (eq 7). The key features of the reaction are presented in Scheme 1. The same detailed mechanism occurs for the second substitution as for the first, but the nature of the first substituent affects the rate of the second step, as discussed below.

The catalytic effect of triethylamine, a non-nucleophilic base, was used to help confirm the mechanism described above. In Table 5, the effect of TEA on the pseudo-first-order rate constants are given for the reactions of DNPO

(24) Acid-Base-Dissociation Constants in Dipolar Aprotic Solvents, IUPAC Commission on Electroanalytical Chemistry, Chemical Data Series No. 35, Blackwell Scientific Publications: Oxford, 1990.

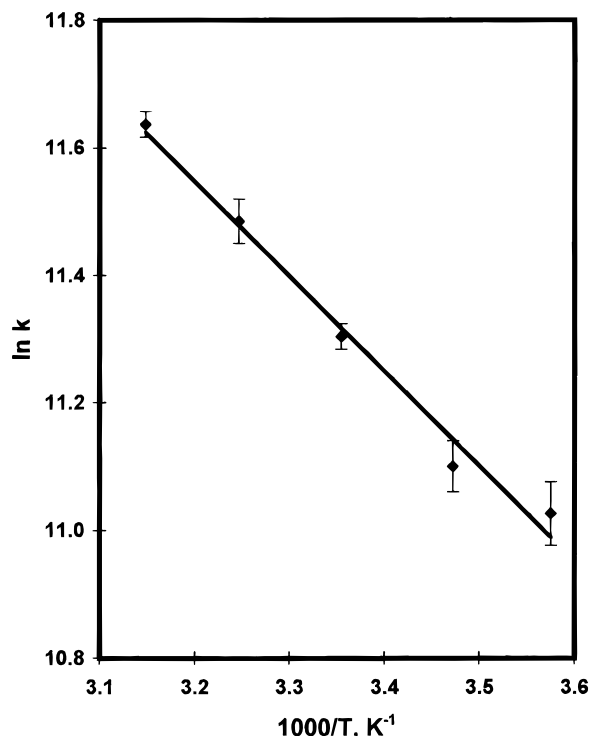
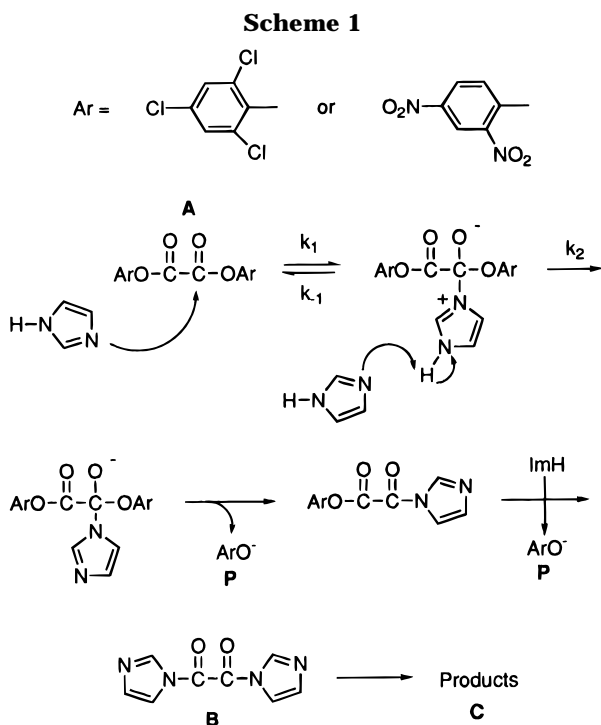


**Figure 7.** Arrhenius plot for the second-order rate constant of the reaction of DNPO with imidazole.



and TCPO with imidazole. The results are consistent with the proposed rate-limiting steps of each reaction. For the reaction of DNPO with imidazole, the effect of TEA is quite small, consistent with the rate-limiting step being addition of ImH to DNPO. For TCPO, however, TEA has a very large effect on the measured rate constant, consistent with TEA accepting a proton from the ImH adduct of TCPO and promoting expulsion of the trichlorophenolate anion ( $k_2$  in eq 4 is accelerated).

This proposed mechanism also explains the differences in temperature dependence for the two reactions. Reactions involving a pre-equilibrium step (eq 7) often have

**Table 5.** Effect of Triethylamine Concentration on the Pseudo-First-Order Rate Constants in the Reaction of Imidazole with TCPO and DNPO. Conditions: 0.10 mM oxalate ester, 5.0 mM Imidazole

[TEA], mM	TCPO: $k_a$ , s <sup>-1</sup>	DNPO: $k_a$ , s <sup>-1</sup>
0	0.216 ± 0.005	100 ± 3
2.50	2.23 ± 0.03	96.8 ± 0.5
5.00	3.26 ± 0.04	103 ± 1
10.0	5.71 ± 0.02	110 ± 3
15.0	9.76 ± 0.05	118 ± 3

low or even negative observed activation energies because of the combination of the temperature dependences of the pre-equilibrium and rate-determining steps of the reaction, as shown below:

$$K_1 = e^{-\Delta G^\ddagger/RT} = e^{\Delta S^\ddagger/R} e^{-\Delta H^\ddagger/RT} \quad (8)$$

$$k_2 = Ae^{-E_a/RT} \quad (9)$$

$$k_{\text{obs}} = k_2K_1 \quad (10)$$

$$k_{\text{obs}} = Ae^{\Delta S^\ddagger/R} e^{-(E_a + \Delta H^\ddagger)/RT} \quad (11)$$

$$E_{a,\text{obs}} = E_a + \Delta H^\ddagger \quad (12)$$

The apparent activation energy,  $E_{a,\text{obs}}$ , is the sum of the enthalpy for formation of the imidazole adduct, which is negative, and the activation energy for the elimination of the phenol, which is positive. If the enthalpy is more negative than the activation energy is positive, the reaction will have an apparent negative activation energy, as was found for the reaction with TCPO.

In the case of DNPO, the addition of ImH ( $k_1$ ) is expected to be more exothermic than for TCPO so that the reverse reaction has a larger energy barrier and is slower. Because DNP is a better leaving group than TCP, the elimination reaction is expected to be faster for DNPO, making the addition step rate-determining. For DNPO, then, the activation energy reflects the barrier to the addition reaction (eq 6). The proposed reaction coordinate diagram given in Figure 8 qualitatively illustrates the differences in the potential energy surfaces for the reactions of TCPO and DNPO with ImH that result in the observed reaction orders and activation energies.

Since the proposed mechanism involves a pre-equilibrium step, experiments were carried out in which the corresponding phenol was added to the reaction mixture in order to determine whether a shift in the position of the equilibrium would affect the reaction rate in the predicted manner; i.e., in the simplest picture one would expect no effect on the DNPO reaction and a decrease in the rate of the TCPO reaction. For the addition of 0.04 mM DNP to 0.02 mM DNPO and 1.0 mM ImH, the reaction rate decreased by approximately 20%. In the reaction of 0.10 mM TCPO with 5.0 mM ImH, the addition of 0.02 mM TCP increased the rate of reaction by approximately 50%. The effect of DNP on the DNPO reaction is quite small (as expected) considering that twice as much DNP was added as DNPO. This result does suggest, however, that the reaction may be partially limited by the establishment of a pre-equilibrium. The effect of TCP on the TCPO reaction gave the opposite effect of that predicted and is probably due to the fact that phenols form strong complexes with their phenox-

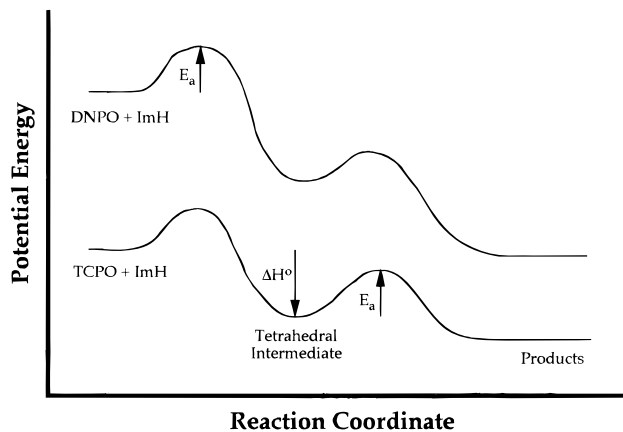


**Figure 8.** Qualitative reaction coordinate diagram for the first substitutions of DNPO and TCPO with imidazole.

ides in aprotic solvents.<sup>25</sup> Thus, the phenol can stabilize the elimination of the phenoxide and speed the decomposition of the tetrahedral intermediate, again consistent with the proposed rate-limiting step in the TCPO reaction with imidazole.

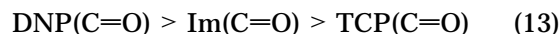
The observations reported here are not without precedent. A dominant second-order dependence on the imidazole concentration has been observed for the imidazole-catalyzed hydrolysis of monocarboxylic acid esters.<sup>26,27</sup> Negative energies of activation have been reported for the aminolysis<sup>28</sup> and imidazole-catalyzed hydrolysis<sup>28</sup> of esters in aprotic solvents. It was postulated that imidazole acts as a nucleophile to form a tetrahedral intermediate whose decomposition is catalyzed by another molecule of imidazole by accepting a proton from the acylimidazolium ion, analogous to our Scheme 1.

The combination of nucleophilic and general-base catalysis was confirmed for diaryl esters in a study of the imidazole-catalyzed hydrolysis of bis(4-nitrophenyl) oxalate, with formation of ODI having a dominant second-order dependence on the imidazole concentration.<sup>16</sup> Finally, a similar second-order dependence, with or without a first-order dependence, on imidazole concentration was observed by Orlovic *et al.* in the imidazole-catalyzed reaction of hydrogen peroxide with TCPO in 75%/25% MeCN–water.<sup>11</sup> Milofsky and Birks observed a second-order dependence on the imidazole concentration in the photoinitiated PO-CL reaction carried out in ethyl acetate.<sup>9</sup>

A difference in the rate-determining step for the imidazole-catalyzed hydrolysis of substituted phenyl ben-

zoates, depending on the nature of the leaving group, was observed in a study by Menegheli *et al.*<sup>29</sup> The rate-determining step for 2,4-dinitrophenyl *p*-nitrobenzoate was addition of imidazole to the acyl carbonyl followed by rapid release of the 2,4-dinitrophenolate ion, as observed here for DNPO. In contrast, the rate-determining step for other benzoates was release of the corresponding phenoxide, as found here for TCPO. A similar dependence of the rate-limiting step on the  $pK_a$  of the leaving group also has been observed for other acyl-transfer reactions.<sup>30,31</sup> Kirsch and Jencks noted that with a good leaving group such as a *p*-nitrophenyl acetate, the uncatalyzed addition of imidazole dominates the kinetics.<sup>31</sup> With less acidic phenols, expulsion of the leaving group becomes more difficult and requires general-base catalysis to stabilize the zwitterionic intermediate. Neuvonen noted both uncatalyzed and general-base catalyzed nucleophilic substitutions of imidazole in reactions with 4-nitrophenyl acetate, chloroacetate, and dichloroacetate.<sup>16</sup> Activation of the acetyl group shifts the reaction from the catalyzed to the uncatalyzed addition of imidazole, again consistent with our observations for TCPO and DNPO.

A final consideration is the relative rates of the first and second substitutions of ImH into TCPO and DNPO. In the case of TCPO, the second substitution appears to be much faster than the first, while for DNPO the second substitution is as much as four times slower. This can be explained if the order of activation by the acyl groups toward substitution on the adjacent carbonyl is



Thus, substitution of ImH for one TCP in TCPO will speed the second substitution, while substitution of ImH for DNP in DNPO will slow the second substitution. This inequality scheme also corresponds to the relative electron withdrawing strengths of the acyl groups.

The results from this study are helpful in explaining the catalytic effects of imidazole on reactions of the two oxalate esters most commonly used for peroxyoxalate chemiluminescence. We are currently investigating the reaction kinetics by observing the chemiluminescence signals under similar reaction conditions, but with hydrogen peroxide and a fluorophore added, in order to further understand the dominant reaction pathways in the PO-CL reaction.

**Acknowledgment.** The stopped-flow instrument was provided by NSF grant BIR-9302748. We thank Shelley Copley for several helpful discussions of this work.

JO951627G

(25) Hadzi, D.; Novak, A.; Gordon, J. E. *J. Phys. Chem.* **1963**, *67*, 1118.

(26) Menger, F. M. *J. Am. Chem. Soc.* **1966**, *88*, 3081.

(27) Su, C.; Watson, J. W. *J. Am. Chem. Soc.* **1974**, *96*, 1854.

(28) Singh, T. D.; Taft, R. W. *J. Am. Chem. Soc.* **1975**, *97*, 3867.

(29) Menegheli, P.; Farah, J. P. S.; Seoud, O. A. E. *Ber. Bunsenges. Phys. Chem.* **1991**, *95*, 1610–1615.

(30) Neuvonen, H. *J. Chem. Soc., Perkin Trans. 2* **1987**, 159.

(31) Kirsch, J. F.; Jencks, W. P. *J. Am. Chem. Soc.* **1984**, *86*, 837.